

# THE EFFECT OF SIZE AND STRESS HISTORY ON FATIGUE CRACK INITIATION AND PROPAGATION

TECHNICAL DOCUMENTARY REPORT NO. ASD-TDR-62-785

August 1962

Directorate of Materials and Processes  
Aeronautical Systems Division  
Air Force Systems Command  
Wright-Patterson Air Force Base, Ohio

Project No. 7351, Task No. 735106

(Prepared under Contract No. AF 61(052)-522 by Prof. Dr. Waloddi Weibull,  
Bockamollan, Brosarps Station, Sweden, author)

## FOREWORD

This report was prepared by Prof. Dr. Waloddi Weibull, Bockamöllan, Sweden under USAF Contract No. AF 61(052)-522. The contract was initiated under Project No. 7351, "Metallic Materials", Task No. 735106, "Behavior of Metals." The contract was administered by the European Office, Office of Aerospace Research. The work was monitored by the Directorate of Materials and Processes, Aeronautical Systems Division, under the direction of Mr. W. J. Trapp.

This report covers work conducted during the period September 1960 to September 1961.

## ABSTRACT

The first part of investigation deals with the effect of size and preloading on the duration  $N_i$  of the crack initiation period. Geometrically similar sheet specimens of two different aluminum alloys were subjected to various load cycles. It was found that each size had its individual S- $N_i$  curve, considerably differing from those of other sizes. A reduction to one and the same size by means of the Neuber stress concentration factor  $K_N$  was only partially successful. A static preload was found to increase the value of  $N_i$  from 11 kc to 205 kc.

The second part of the investigation deals with the propagation period. Equations relating crack length to number of cycles are derived for two alternatives: constant stress cycle and constant load cycle applied to a sheet specimen. The formulas are verified by tests including various combinations of material, size, and stress amplitude.

In the first alternative, it was found that the rate of crack growth is, independently of the crack length, constant after a transition period had been passed. The duration of this period is dependent on the duration of the preceding initiation period. For small values of  $N_i$  it does not even exist.


In the second alternative a convenient method for interpreting the results was obtained by plotting crack length vs. number of cycles. It was found that the propagation period starts with a transition period, followed by one, two, or even three stable propagation periods, the number depending on the magnitude of the applied load. An examination of the broken specimens showed that these periods correspond to different fatigue mechanisms.

It is concluded that total fatigue life cannot be predicted without considering separately the parts of which it is composed. Consequently, it cannot be expected that the shape of the conventional S-N curve that relates total life to applied load can be corrected to relevant testing conditions.

## PUBLICATION REVIEW

This report has been reviewed and is approved.

FOR THE COMMANDER:



W. J. TRAPP  
Chief, Strength and Dynamics Branch  
Metals and Ceramics Laboratory  
Directorate of Materials and Processes

## TABLE OF CONTENTS

	PAGE
I. INTRODUCTION . . . . .	1
II. CRACK INITIATION . . . . .	1
III. CRACK PROPAGATION . . . . .	3
3.1 Derivation of Equations Relating Crack Length to Number of Cycles . . . . .	3
3.2 Experimental Verification of the Formulas . . . . .	5
a. Constant Stress Cycle . . . . .	5
b. Constant Load Cycle . . . . .	6
3.3 Comparison with Results of Frost and Dugdale . . . . .	7
3.4 Comparison with Results of Illg and McEvily . . . . .	8
IV. CONCLUDING REMARKS . . . . .	8
V. REFERENCES . . . . .	9

## LIST OF FIGURES

FIGURE		PAGE
1.	S- $N_i$ Curves for Geometrically Similar Specimens of 24S-T . . . . .	10
2.	Crack Length Vs. Number of Cycles for Geometrically Similar Specimens of 24S-T; $\sigma_x = \sigma_i = 12.0 \text{ kg/mm}^2$ . . . . .	11
3.	Crack Length Vs. Number of Cycles for Geometrically Similar Specimens of 75S-T, Alclad; $\sigma_x = \sigma_i = 12.0 \text{ kg/mm}^2$ . . . . .	11
4.	Relative Crack Length Vs. Number of Cycles Plotted on Linear and Semi-logarithmic Scales. Mat. 75S-T, Alclad; $\sigma_x = \sigma_i = 12.0 \text{ kg/mm}^2$ . . . . .	12
5.	Series 12.150.15.2x; $N_i = 2.6 \text{ kc}$ and Series 12.170.2, 4.2s $\ell$ ; $N_i = 35.9 \text{ kc}$ ; Mat. 24S-T. . . . .	12
6.	Series 7.0/170.6/12.1/2x; $N_i = 9.0 \text{ kc}$ ; Mat. 24S-T . . . . .	13
7.	Series 7.0/170.6/12.1/2x; Component 1 . . . . .	14
8.	Series 7.0/170.6/12.1/2x Plotted on Linear Scales . . . . .	15
9.	Two Series with Different Size of Notch . . . . .	16
10.	Series 7.0/170.6/12.1/2x without and with Preload ( $3 \times 15.0 \text{ kg/mm}^2$ ) Plotted on Linear Scales. Mat. 24S-T . . . . .	17
11.	Series 7.0/170.6/12.1/2x Preload; $\sigma_i = 8.0$ , $N_i = 204 \text{ kc}$ . . . . .	18
12.	Series 7.0/170.6/12.1/2x Preloaded; Components 1, 2, and 3 . . . . .	19
13.	Series 3.5/170.6/12.1/2x; $\sigma_i = 4.0$ , $N_i = 3,084 \text{ kc}$ . Mat. 24S-T . . . . .	20
14.	Series 5.5/45.0/12.2/2x; $\sigma_i = 6.3$ , $N_i = 280 \text{ kc}$ . Mat. 24S-T . . . . .	21
15.	Series 11.8/170.6/1.4/2 s $\ell$ Plotted on $\log x \div N$ Scales. Mat. 24S-T . . . . .	22
16.	Series 7.0/304.8/1.0/2 s $\ell$ . Data from Illg and McEvily, NASA TN D-52, Mat. 2024-T3, $S_o = 6.00 \text{ ksi}$ , $R = -1$ . . . . .	23

LIST OF TABLES

TABLE NR.		PAGE
I	Size Effect on Crack Initiation ( $N_i$ ) in Geometrically Similar Specimens at Various Stress Levels. Material: 24S-T . . . . .	2
II	Size Effect on Total Life ( $N_B$ ), Initiation ( $N_i$ ), and Propagation ( $N_p$ ) in Geometrically Similar Specimens at $\sigma_i = 8.0 \text{ kg/mm}^2$ . Material: 24S-T . . . . .	2

## I. INTRODUCTION

The main purpose of the present investigation was to demonstrate that the macro-stage of the fatigue process (to use the nomenclature of Schijve<sup>(1)</sup>), starting with a crack visible with the naked eye and ending with final rupture, is itself a complex process composed of several periods. Since each of these periods is strongly and differently affected by the size of the specimen and the stress history preceding it, no prediction of the total life of the specimen can be done without due consideration to this fact. It is felt that this neglect may be the real cause of many controversial conclusions.

When the crack starts growing, the fatigue test can be continued in two different ways:

The load is reduced in proportion to the remaining cross-sectional area, giving a constant stress cycle, and

the initial load cycle is kept constant, resulting in a successively increasing stress cycle.

Mathematical formulas for the crack propagation applicable to both alternatives have been derived. Since they are based on the assumption that the rate of propagation is independent of the crack length, which stands in opposition to existing theories, it appeared necessary to confront the formulas not only with results from test series designed for this purpose and carried out at the Aeronautical Research Institute of Sweden (FFA) under the supervision of G. Wällgren, but also with those presented by other investigators. Two extensive and careful investigations have been examined, viz., one by Frost and Dugdale<sup>(5)</sup>, who assume that the rate is proportional to the crack length, and another by Ilg and McEvily<sup>(6),(7)</sup>, who assume that the rate is proportional to (crack length)<sup>3/2</sup>, as originally proposed by Head.

## II. CRACK INITIATION

The number of cycles,  $N_i$ , at the appearance of the first crack in the aperture of geometrically similar 24S-T sheet specimens of four different sizes subjected to various stress amplitudes ( $R = 0$ ) have been measured. The result is presented in Table I. The shape of the specimens and the testing conditions are specified in Refs. (2), (3), and (4).

It is obvious that the size effect on  $N_i$  is considerable. The results show that each size has its own individual  $S-N$  curve as demonstrated in Figure 1. This family of curves, as based on twenty-one tests only, is preliminary and has to be completed, but the small scatter observed indicates that only a moderate number of tests will be required for attaining a sufficient accuracy.

---

Manuscript released by author 15 September 1961 for publication as an ASD Technical Report.

Table I

Size Effect on Crack Initiation ( $N_i$ ) in Geometrically Similar Specimens at Various Stress Levels. Material: 24S-T.

$\sigma_i$ kg/mm <sup>2</sup>	w = 22.8 mm		w = 45.5 mm		w = 68.3 mm		w = 170.6 mm	
	$N_i$		$N_i$		$N_i$		$N_i$	
	n	kc	n	kc	n	kc	n	kc
12.0	3	36.0	-	-	2	4.0	1	2.6
10.2	-	-	2	19.0	-	-	-	-
8.0	3	1,205.0	3	50.7	2	19.5	2	11.0
6.3	-	-	1	280.0	-	-	-	-
4.0	-	-	-	-	2	974.0	-	-

n = number of observations

An attempt to reduce the applied stresses to one and the same size (170.6) by means of the Neuber stress-concentration factor  $K_N$  (cf. Ref. (6), Appendix) was successful for the size 68.3 only, as shown in Figure 1, while the corrections for the sizes 20.8 and 45.5 were too small. Assuming the material constant  $\rho'$  to be 0.003 in. = 0.076 mm, the values of  $K_N$  are 4.92, 5.68, 6.10, and 7.04, respectively. The arrows indicate the corresponding shift of the curves. Tentatively, it is proposed that the remaining correction of the two upper curves may be obtained by means of the statistical theory of strength.

It is of interest to note that there is a considerable size effect also on the duration of the propagation  $N_p$ , and on the ratio  $N_i/N_B$  as shown in Table II. These

Table II

Size Effect on Total Life ( $N_B$ ), Initiation ( $N_i$ ), and Propagation ( $N_p$ ) in Geometrically Similar Specimens at  $\sigma_i = 8.0$  kg/mm<sup>2</sup>. Material: 24S-T.

w mm	$N_B$ kc	$N_i$ kc	$N_p$ kc	$N_i/N_B$ %	
22.8	2,007	1,100	907	54.8	} 60.3
22.8	2,644	1,200	1,444	54.6	
22.8	1,838	1,315	523	71.5	
45.5	470	60	410	12.8	} 10.6
45.5	395	33	362	8.4	
170.6	147	13	134	8.8	} 7.4
170.6	150	9	141	6.0	



effects are very complicated and require, as will be demonstrated in the sequel, a closer examination of the propagation period and its dividing into subperiods.

The effect of the stress history on  $N_i$  will be illustrated by a single test result. After preloading a specimen of size 170.6 three times with a static stress of  $15.0 \text{ kg/mm}^2$ , the initiation time increased from  $N_i = 11 \text{ kc}$  to  $N_i = 205 \text{ kc}$ . This result is more closely analyzed in the following paragraph.

### III. CRACK PROPAGATION

#### 3.1 Derivation of Equations Relating Crack Length to Number of Cycles

The following symbols are used:

a = total width of central aperture, mm

d = diameter of central hole, mm

$l_1, l_2$  = crack length measured from center of specimen, mm

s = net width of specimen, mm

t = sheet thickness, mm

w = total width of specimen, mm

x =  $(l_1 + l_2)/w$ , %

$x_i$  =  $a/w$ , %

L = applied maximum load within a cycle, kg

R = stress ratio =  $L_{\min}/L$

A = area,  $\text{mm}^2$

$\sigma$  =  $L/A$ ,  $\text{kg/mm}^2 = 1.422 \text{ ksi}$

$\sigma_0$  =  $L/w \cdot t$

$\sigma_i$  =  $\sigma_0/(1 - x_i)$

$\sigma_x$  =  $\sigma_0/(1 - x)$

N = number of cycles measured from start of test, kc

$N_i$  = number of cycles at appearance of a visible crack

$N_B$  = number of cycles at final rupture ( $x = 100\%$ )

$N_0$  = number of cycles extrapolated to  $x = 0$

$$N_p = N_B - N_i; N_1 = N_B - N_o; N_x = N - N_o; N_{xi} = N_i - N_o$$

A test run with constant stress cycle, is specified by a Code:  $\sigma_i . s . d . t$  to which is added  $x$ , if the aperture is a notched circular hole, and  $sl$ , if the aperture is a slit.

A test run with constant load cycle, is specified by a Code  $\sigma_o/w/x_i/t$  with addition of  $x$  or  $sl$ .

A propagation equation will now be derived on the basis of the three following assumptions:

- (i) The rate of growth is independent of the crack length
- (ii) There is a parabolic relationship between the relative rate of growth,  $dx/dN$ , and an effective stress at the tip of the crack,
- (iii) There is a parabolic relationship between the effective stress at the tip and the nominal stress based on the remaining cross-sectional area.

Combining (ii) and (iii) we have

$$dx/dN = k . \sigma_x^\beta . \quad \text{Equ. 1}$$

In the case of constant stress cycle we then have, since  $\sigma_x = \sigma_i = \text{constant}$ ,

$$d\ell/dN = k . w . \sigma_i^\beta \quad \text{Equ. 2}$$

and

$$\ell = k . w . \sigma_i^\beta . N . \quad \text{Equ. 3}$$

In the case of constant load cycle we have

$$\sigma_x = \sigma_o/(1 - x) \quad \text{Equ. 4}$$

where  $\sigma_o = \text{constant}$  and thus

$$dx/dN = k . \sigma_o^\beta / (1 - x)^\beta \quad \text{Equ. 5}$$

and after integration

$$(1 - x)^{\beta + 1} = k(\beta + 1)\sigma_o^\beta (N_B - N) . \quad \text{Equ. 6}$$

Introducing

$$N_1 = 1/k(\beta + 1)\sigma_o^\beta \quad \text{Equ. 7}$$

it follows that

$$(1 - x)^{\beta + 1} = (N_B - N)/N_1. \quad \text{Equ. 8}$$

Since, by definition,

$$N_1 - N_x = N_B - N \quad \text{Equ. 9}$$

we have

$$(1 - x)^{\beta + 1} = 1 - N_x/N_1. \quad \text{Equ. 10}$$

This equation involves two parameters only,  $\beta$  and  $N_1$ .

From Equation 8 it follows that

$$(\beta + 1) \log (1 - x) = \log (N_B - N) - \log N_1. \quad \text{Equ. 11}$$

If a test is terminated before failure occurs, the value of  $N_B$  is unknown, but it can be defined as that value that rectifies the curve. This method of determining  $N_B$  is very sensitive, if the last observed value of  $N$  does not differ much from  $N_B$ . It has to be used also when there are two or more components of the  $x - N$  curve, as will be demonstrated below.

### 3.2 Experimental Verification of the Formulas

#### a. Constant Stress Cycle

In this particular case Equation 3 is valid. If then  $\ell$  is plotted against  $N$  a straight line will result with a slope that for a given  $\sigma_i$  is proportional to the width  $w$ .

Figure 2 shows the result for the Material 24S-T,  $\sigma_i = 12.0 \text{ kg/mm}^2$ , and four different sizes, and Figure 3 the result for the Material 75S-T,  $\sigma_i = 12.0 \text{ kg/mm}^2$ , and three different sizes. More examples of the linear relationship between  $\ell$  and  $N$  may be found in Refs. (3) and (4). Its validity even for cracks approaching the edge of the specimen is demonstrated by Figure 4. There is no doubt that sufficiently small intervals of changing the load would carry the straight line still closer to the edge.

It was observed that in cases where the value of  $N_i$  is small the straight line starts immediately, while there is for large values of  $N_i$  a transition period, during which the rate of growth increases continuously until a stable rate is attained. Since the duration of the transition period can be deliberately changed by applying preloads or prestresses to the specimen and since it depends on the duration of the initiation period, it is felt that this period is not a matter of geometry but of the stress history prior to the end of the initiation period. Figure 5 illustrates this statement. The values were  $N_i = 2.6 \text{ kc}$  and  $N_i = 35.9 \text{ kc}$ , respectively. The only difference between the specimens was the width of the aperture, which caused the difference in  $N_i$ . In the first case the stable propagation started immediately, in the second case after more than 200 kc.

## b. Constant Load Cycle

In this particular case, Equation 11 is supposed to be valid and straight lines are expected when plotting  $\log(1-x)$  against  $\log(N_B - N)$ . As shown in Figure 6 this expectation is nicely satisfied for  $x > 40\%$ .

At  $x = 41.4\%$  there is a marked discontinuity in the curve, which thus involves two components. The lower part of the line is curved, but it can be rectified by using the value  $N_B = 294.7$  kc instead of the observed value 286.5 kc, which is valid for the upper part. The result is demonstrated in Figure 7. The dotted line represents a replicated test. The differences in  $N_i$ ,  $\beta$ , and  $N_1$  are small. (The two values of  $N_1$  correspond to the left- and right-hand cracks.)

Observed values of this test series are in Figure 8 plotted on linear  $x - N$  scales and also the theoretical curve corresponding to Equation 8, which fits the data point very nicely indeed. This way of plotting makes it difficult to detect that the curve actually consists of two components.

It seemed reasonable to assume that the discontinuity in the curve indicates a change in the damaging process. An examination of the broken specimen confirms this assumption. For crack lengths smaller than 25 mm = 41.4% the crack has grown at  $90^\circ$  to the plane of the sheet but above this length fracture occurs on a plane inclined at  $45^\circ$  to the plane of the sheet. This observation has previously been made by Frost and Dugdale (5) who, however, did not find any distinct change in the rate of growth at the transition point, probably owing to a less precise method of measuring the rate.

Similarly, Shabal'm(8) found that in rotating bending the failure occurs at an angle of  $45^\circ$  to the axis of the circular specimen at high stress levels, while at low stresses the failure occurs in the plane of maximum normal stresses.

Assuming that the change in the mode of fracture occurs at a certain stress amplitude, it is expected that there will be only one component at sufficiently high values of  $\sigma_1$ , but otherwise two or three components. Figure 9 confirms this expectation. The difference between the two specimens is the width of the central aperture, giving  $\sigma_1 = 12.2$  and  $10.9$  kg/mm<sup>2</sup>, respectively. In the first case, the failure occurs at  $45^\circ$ , while in the second case, the crack starts at  $90^\circ$ , followed by a double shear, and finally by a single shear failure (not included in the curve). It is not clear whether the higher value  $\sigma_{12} = 13.6$  kg/mm<sup>2</sup> instead of 11.9 is a sampling deviation or due to the different stress history.

In the preceding diagrams no transition period was observed, probably because of the small values of  $N_i$ . For this purpose it was of interest to find out whether it was possible to produce a transition period by applying a preload to the specimen. The test presented in Figure 6 was replicated after having imposed on an identical specimen three times a static load producing a maximum stress of 15.0 kg/mm<sup>2</sup>. The result is demonstrated in Figure 10. The most striking feature is the change in  $N_i$  from 11 kc to 205 kc. By shifting the preloaded curve 194 kc to the left, it becomes apparent that the preload has improved the fatigue properties in the earlier part but has deteriorated them in the later part of the curve. The total effect was a nonsignificant decrease of  $N_p$  from 139 to 134 kc.

The linear plotting used in Figure 10 gives no indication that the damaging process in this particular case involves five distinct macro-stages, which, however, are easily detected by plotting the observations on  $\log(1-x) \div \log(N_B - N)$  scales, as done in Figure 11. The initiation period ends at  $N_i$ , the transition period ends at  $N_t$ , and three stable propagation periods end at  $N_{12}$ ,  $N_{23}$ , and  $N_B$ , called components 1, 2, and 3. They are presented with more details in Figure 12. (Values within parentheses correspond to the virgin specimen.) It is found that the stress at the transition point  $x_{12}$  has changed from 11.9 to 11.3, which is insignificant. The only significant change in components 1 and 2 is a deterioration in  $N_1$  from 286 kc to 176 kc in the first component. Component 3 was not observed in the test with the virgin specimen.

Examination of the broken specimen reveals three different modes of fracture: tensile, double shear, and single shear.

The influence of the initiation period on the propagation will now be illustrated by two examples:

In Figure 13 the initiation period is specified by  $\sigma_i = 4.0 \text{ kg/mm}^2$ ;  $N_i = 3,084 \text{ kc}$ . This very long period has produced a transition period ending at  $x_t = 34\%$ . Observations included in the curve correspond to a tensile mode of fracture, while the broken specimen reveals a change-over to single shear failure at large crack lengths.

In Figure 14 the initiation period is specified by  $\sigma_i = 6.3 \text{ kg/mm}^2$ ;  $N_i = 280 \text{ kc}$ . The transition period ends at  $x_t = 58\%$ . Since the stress  $\sigma_t = 13.1 \text{ kg/mm}^2$ , it seems plausible to assume that the transition period has swallowed up the first component. The specimen was not available for inspection.

### 3.3 Comparison with Results of Frost and Dugdale

In the paper by Frost and Dugdale<sup>(5)</sup> it was postulated that the rate of growth, using the present symbols, is

$$d\ell/dN = k \cdot \sigma_0^n \cdot 1 \quad \text{Equ. 12}$$

or, dividing by  $w$ ,

$$dx/dN = k \cdot \sigma_0^n \cdot x \quad \text{Equ. 13}$$

for values of  $x$  less than  $1/8$ .

Hence,

$$\log(x/x_i) = k_0 \cdot N. \quad \text{Equ. 14}$$

Consequently, if  $\log x$  is plotted against  $N$  a straight line should be obtained. Results presented in the paper confirms this assumption very nicely.

However, these results can be interpreted in a quite different way, as demonstrated by plotting a curve corresponding to Equation 8 on  $\log x \div N$  scales. Taking the result from a test, defined by the code: 11.8/170.6/1.4/s $\ell$  the

theoretical curve and the observations plot as demonstrated in Figure 15. The shape of this curve shows that no experimental decision between the two theories can be made by means of crack lengths larger than 5%. (Equation 12 is not claimed to be valid for  $x > 12.5\%$ .) In this particular test the two lowest observed values deviate significantly from the straight line postulated by Frost and Dugdale, due to the fact that no transition period was involved as a consequence of the small value  $N_i = 29.5$  kc. If, however, a transition period is involved, then the rate of growth will start from a low initial value and continuously increase, as illustrated, for instance, in Figures 11, 13, and 15 until the stable propagation period is reached. This effect will straighten the initial part of the curve plotted on  $\log x \div N$  scales, thus simulating a curve expected according to the theory of Frost and Dugdale. No values of  $N_i$  are given in the paper, but, considering the small dimensions of the central slit, it seems safe to assume that the initiation periods were long, and so it is felt that these tests have, in fact, been restricted to the transition period of the propagation.

### 3.4 Comparison with Results of Illg and McEvily

Some of the data from Refs. (6) and (7) have been plotted on  $\log(1-x) \div \log(N_B - N)$  scales. In all cases examined, transition periods have been observed, particularly long when the crack was initiated by means of stresses higher than those applied during the propagation. This result was expected because of the small dimensions of the central slit.

A curve with a relatively short transition period is shown in Figure 16. The transition period ends at  $x_c = 10\%$ . The following observations very exactly plot on a straight line. Since the test was terminated at a stress  $\sigma = 10.5$  kg/mm<sup>2</sup>, no indication of a component 2 was expected.

It is of interest to note that the specimen was subjected to completely reversed loading.

## IV. CONCLUDING REMARKS

### *CONCLUSIONS*

The results accomplished are based on fatigue tests applied to sheet specimens notched by a central aperture. It is believed that the sequence of macro-stages observed is not restricted to this particular type of specimen. On the contrary, it is felt that any fatigue process is composed of one initiation period, in many cases followed by a transition period, and one or more stable propagation periods.

Since these various periods are influenced not only by the preceding ones but also, and in completely different ways, by various factors, it is concluded that the total fatigue life cannot be predicted with any confidence without considering separately the parts of which it is composed. Consequently, it cannot be expected that the shape of the conventional S-N curve (the Wöhler curve) that relates total life to applied load can, by simple laws, be correlated to relevant testing conditions, an aspiration more likely realizable, if applied to the S-N<sub>i</sub>, S-N<sub>a</sub>, and S-N<sub>12</sub> curves.

## V. REFERENCES

- (1) Schijve, J. Fatigue Crack Propagation in Light Alloys. NLL Report M.2010. July 1956.
- (2) Weibull, W. The Propagation of Fatigue Cracks in Light-Alloy Plates. SAAB TN 25, January 1954.
- (3) Weibull, W. Effect of Crack Length and Stress Amplitude on Growth of Fatigue Cracks. FFA Report 65, Stockholm, May 1956.
- (4) Weibull, W. Size Effects on Fatigue Crack Initiation and Propagation in Aluminum Sheet Specimens Subjected to Stresses of Nearly Constant Amplitude. FFA Report 86, June 1960.
- (5) Frost, N. E. and Dugdale, D. S. The Propagation of Fatigue Cracks in Sheet Specimens. J. Mech. Phys. Solids 6, 92-110, 1958.
- (6) McEvily, A. J. and Illg, W. The Rate of Fatigue-Crack Propagation in Two Aluminum Alloys. NASA TN 4394, September 1958.
- (7) Illg, W. and McEvily, A. J. The Rate of Fatigue-Crack Propagation for Two Aluminum Alloys under Completely Reversed Loading. NASA TN D-52, October 1959.
- (8) Shabalin, V. J. On the Discontinuity in Fatigue Curves of Duralumin. J. Techn. Phys. (Russian). 1022-1024. May, 1958.

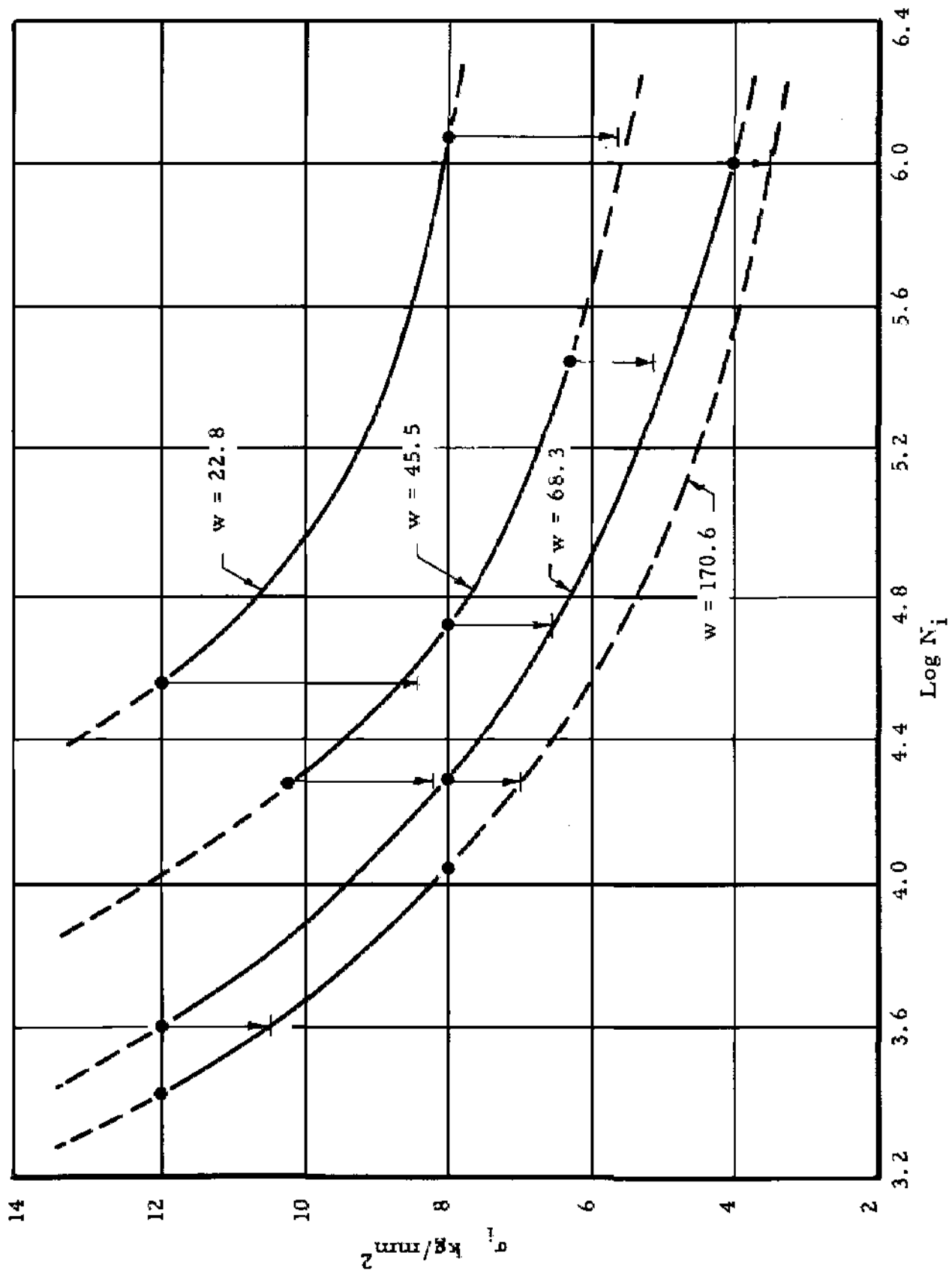


Figure 1. S- $N_i$  Curves for Geometrically Similar Specimens of 24S-T



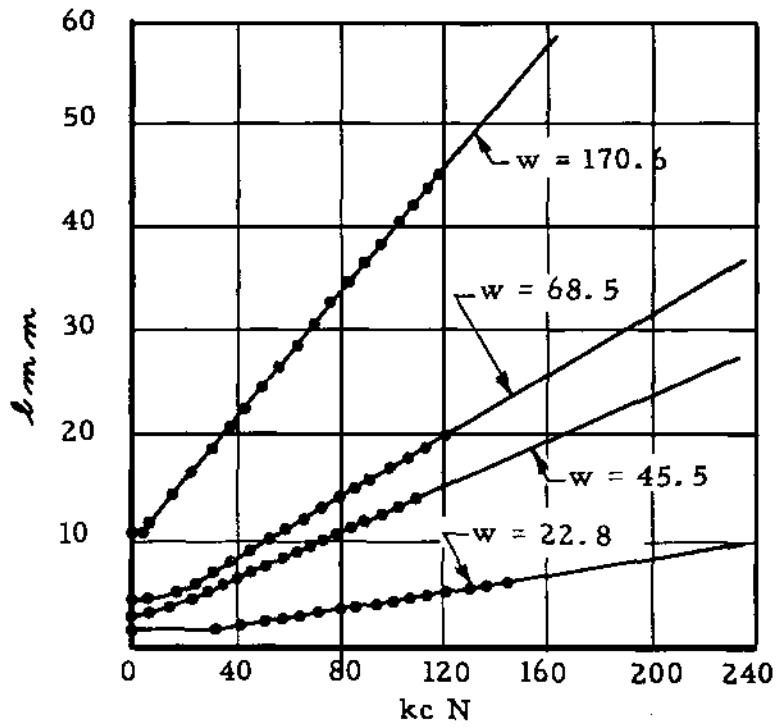


Figure 2. Crack Length vs. Number of Cycles for Geometrically Similar Specimens of 24S-T;  $\sigma_x = \sigma_i = 12.0 \text{ kg/mm}^2$

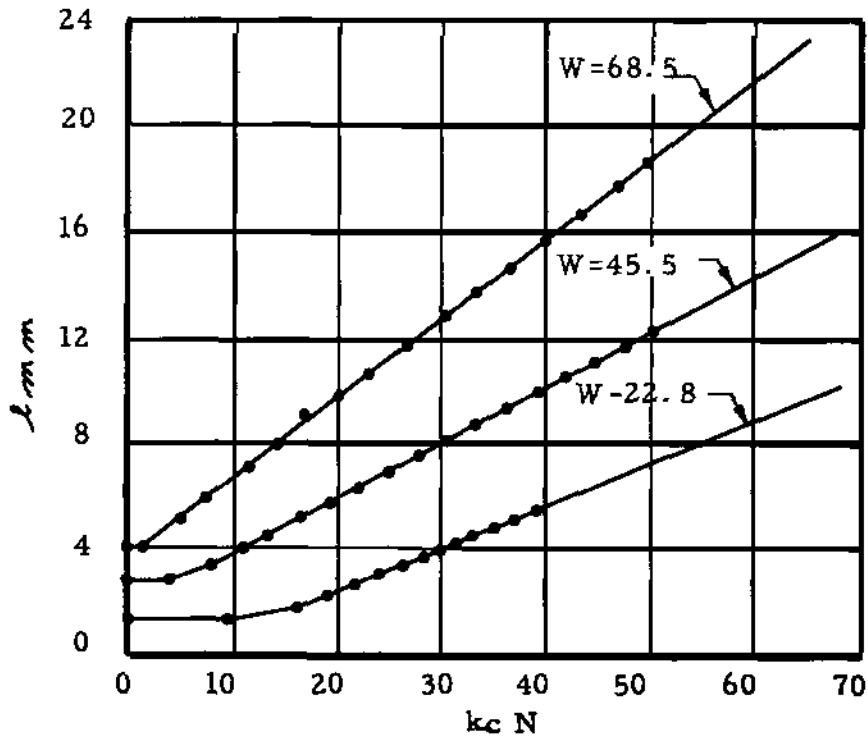


Figure 3. Crack Length vs. Number of Cycles for Geometrically Similar Specimens of 75S-T, Alclad;  $\sigma_x = \sigma_i = 12.0 \text{ kg/mm}^2$

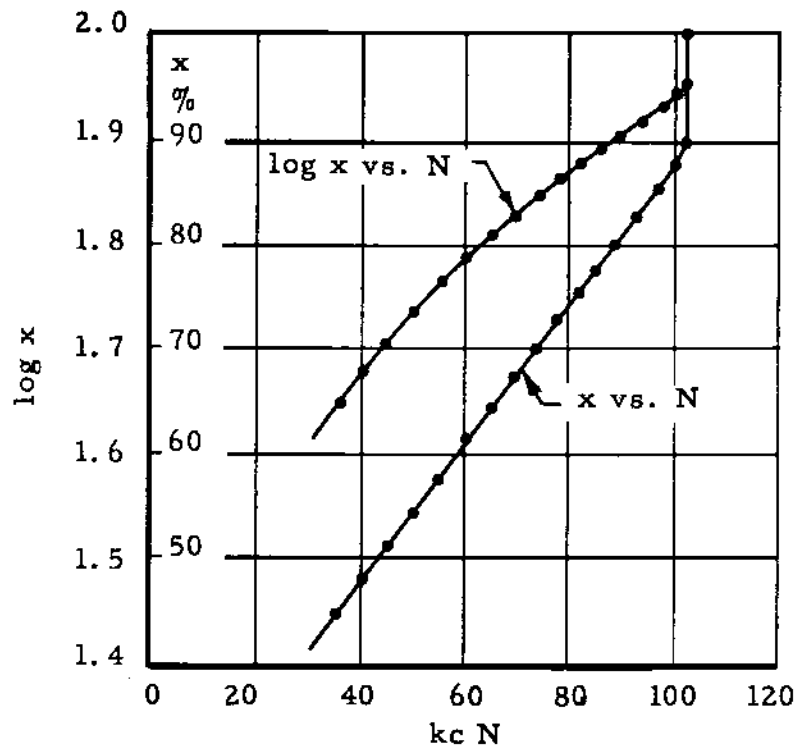


Figure 4. Relative Crack Length vs Number of Cycles Plotted on Linear and Semi-logarithmic Scales. Mat. 75S-T, Alclad;  $\sigma_x = \sigma_i = 12.0 \text{ kg/mm}^2$

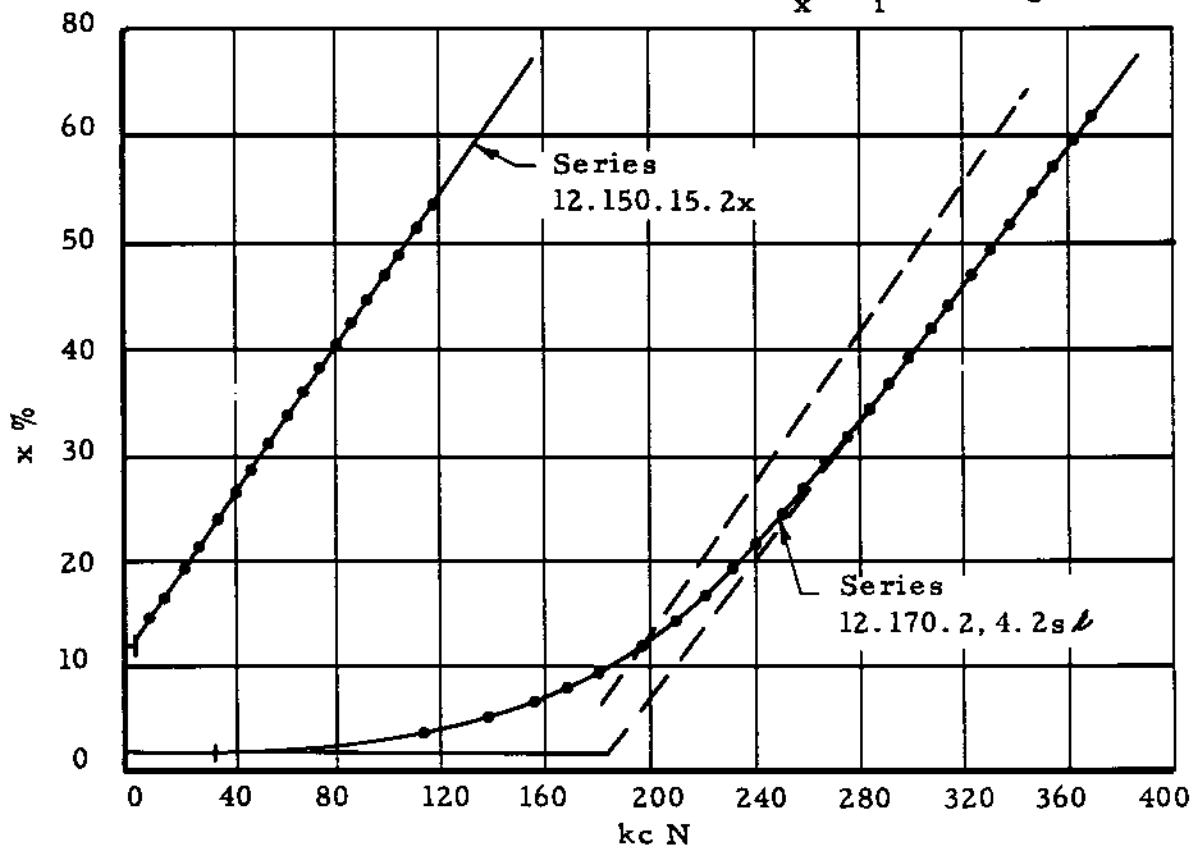


Figure 5. Series 12.150.15.2x;  $N = 2.6 \text{ kc}$  and Series 12.170.2, 4.2s;  $N_i = 35.9 \text{ kc}$ ; Mat. 24S-T.

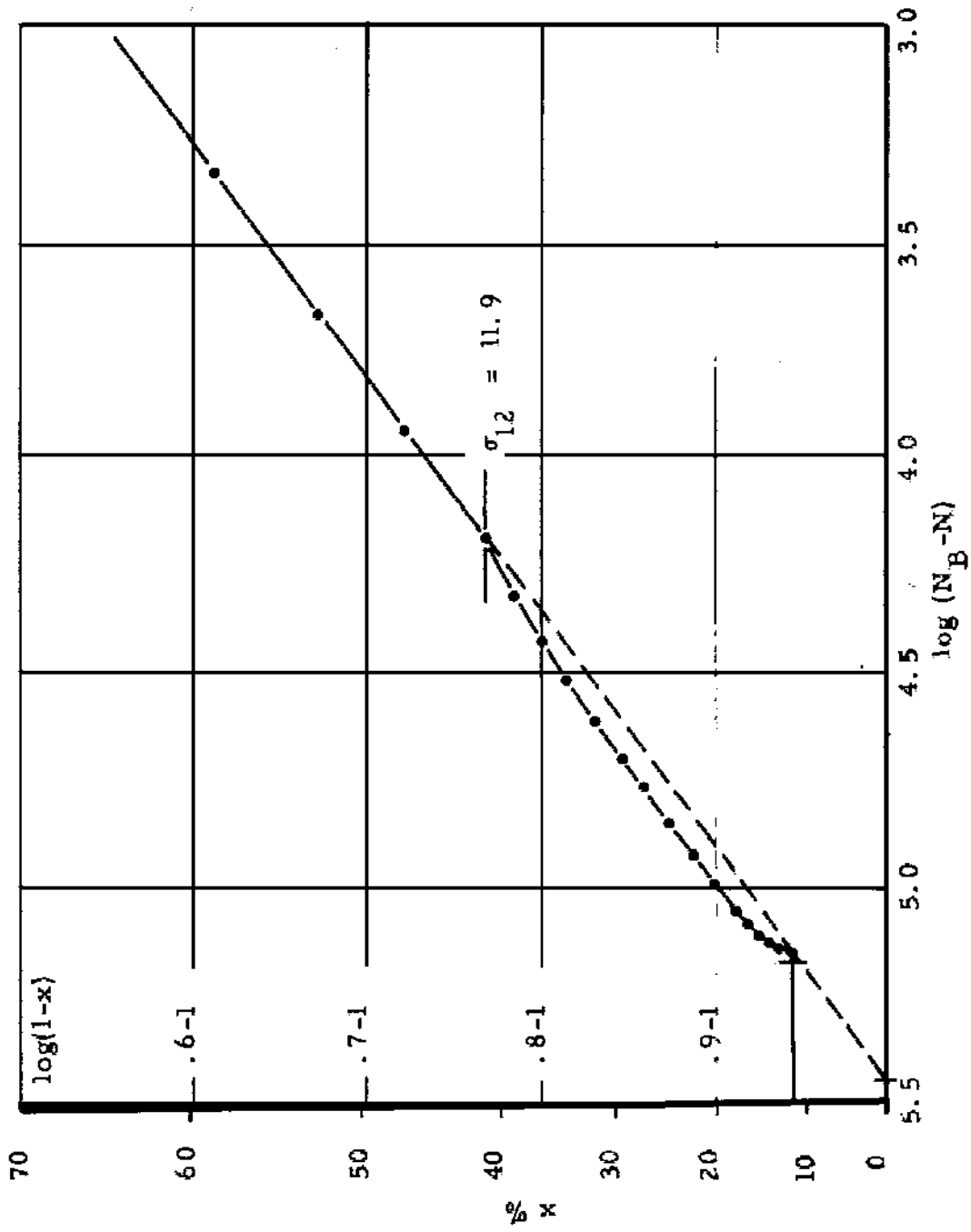


Figure 6. Series 7.0/170.6/12.1/2x; N<sub>1</sub> = 9.0 kc; Mat. 24S-T

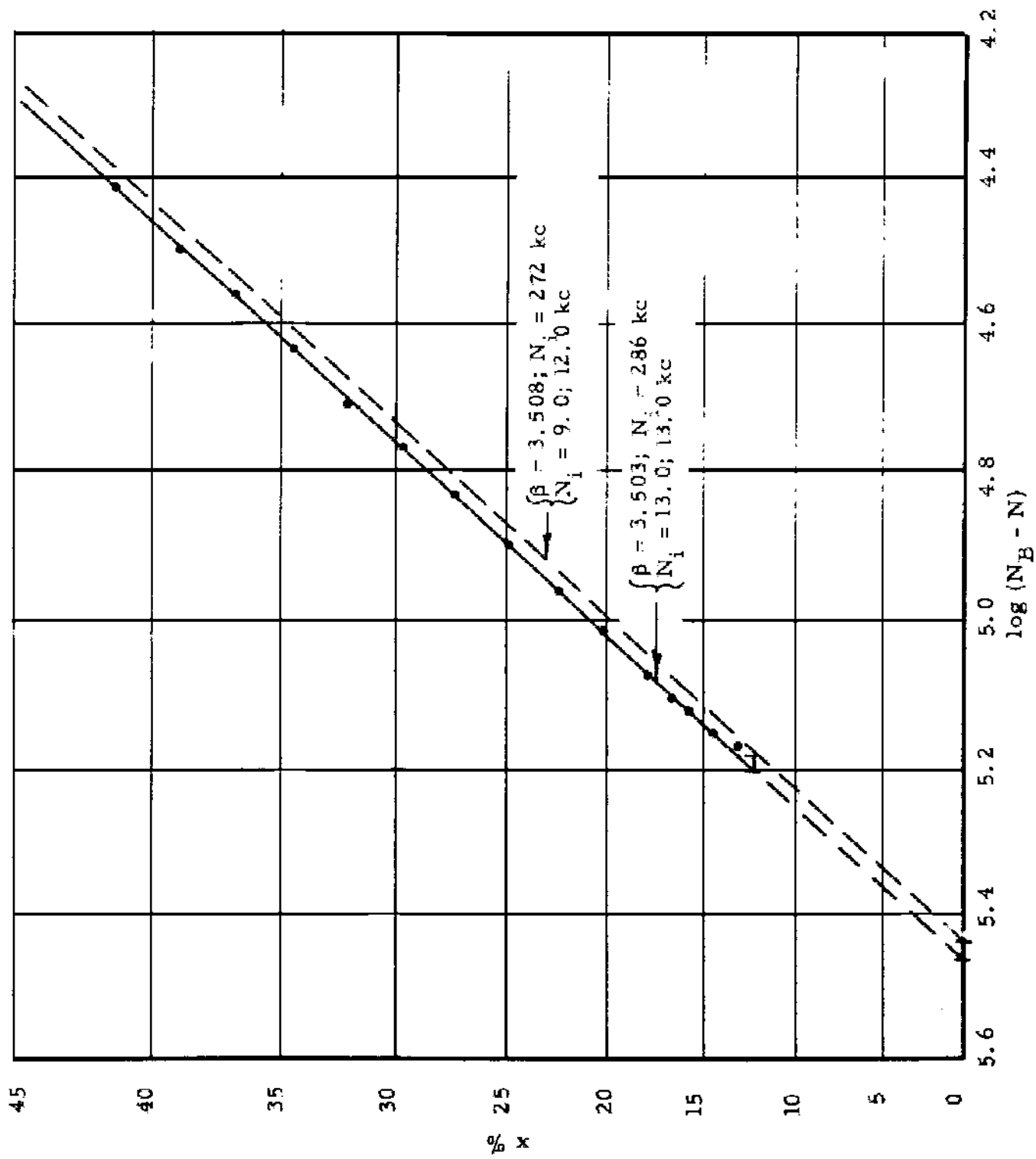


Figure 7. Series 7.0/170.6/12.1/2x; Component 1

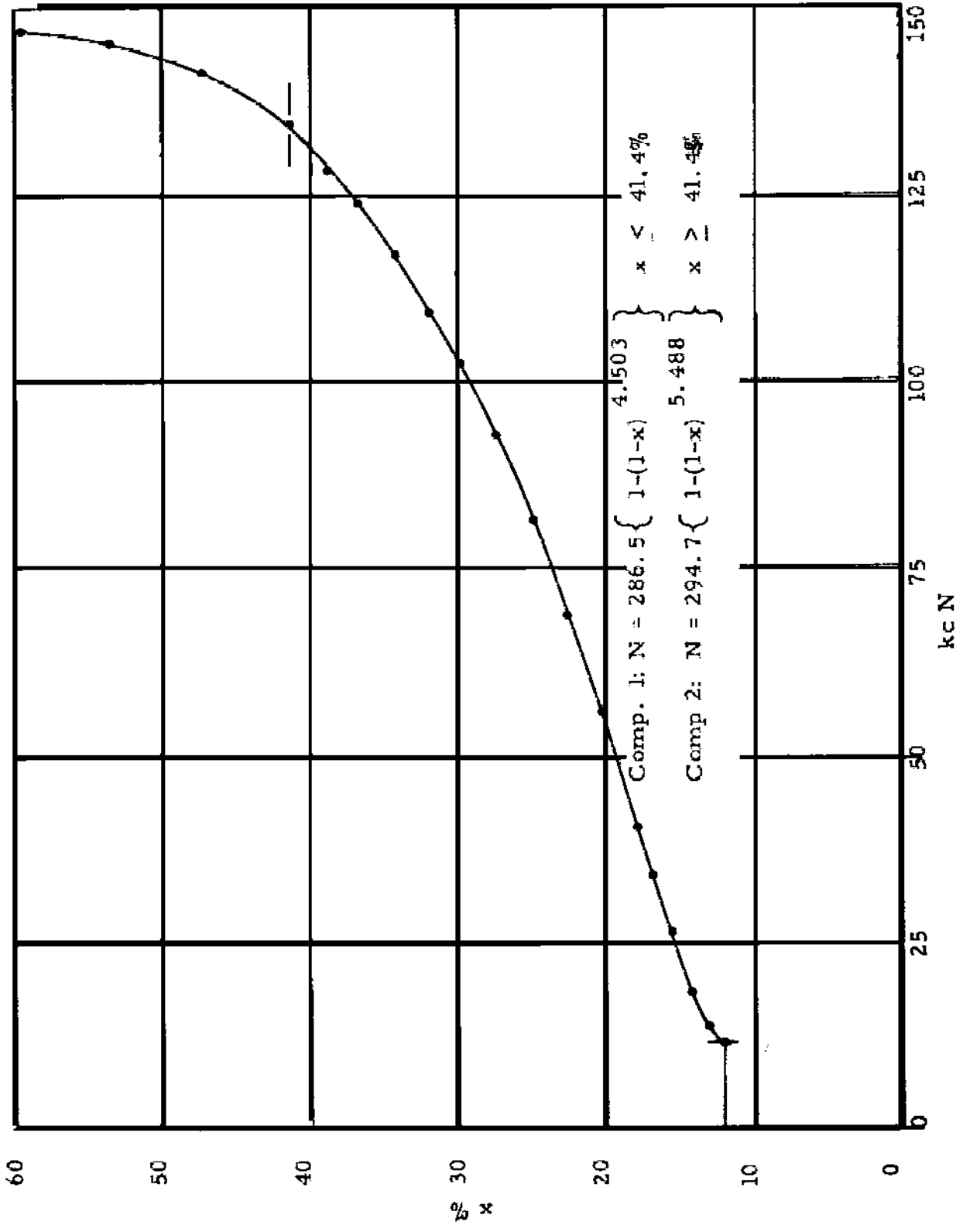


Figure 8. Series 7.0/170.6/12.1/2x Plotted on Linear Scales

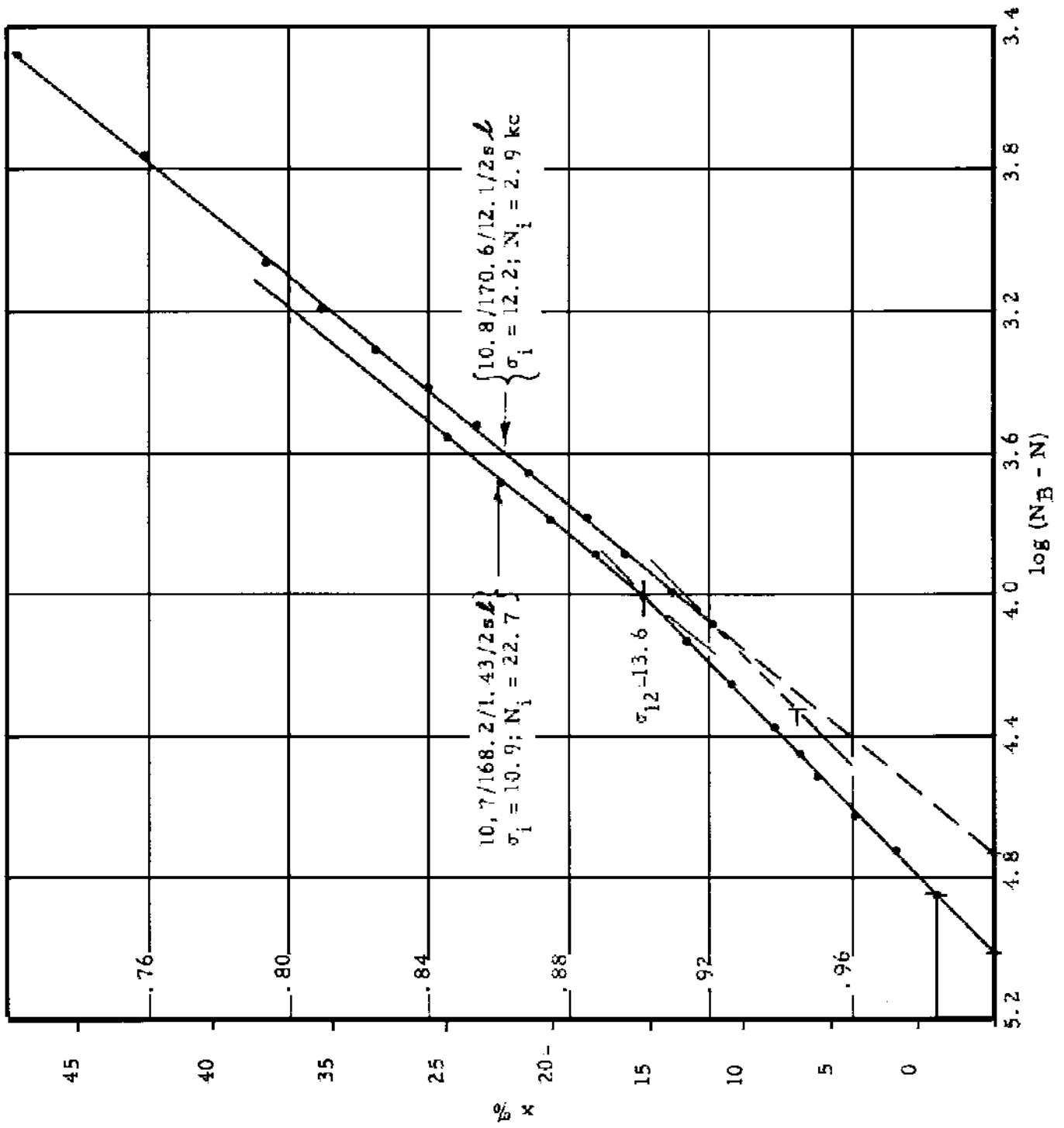


Figure 9. Two Series with Different Size of Notch

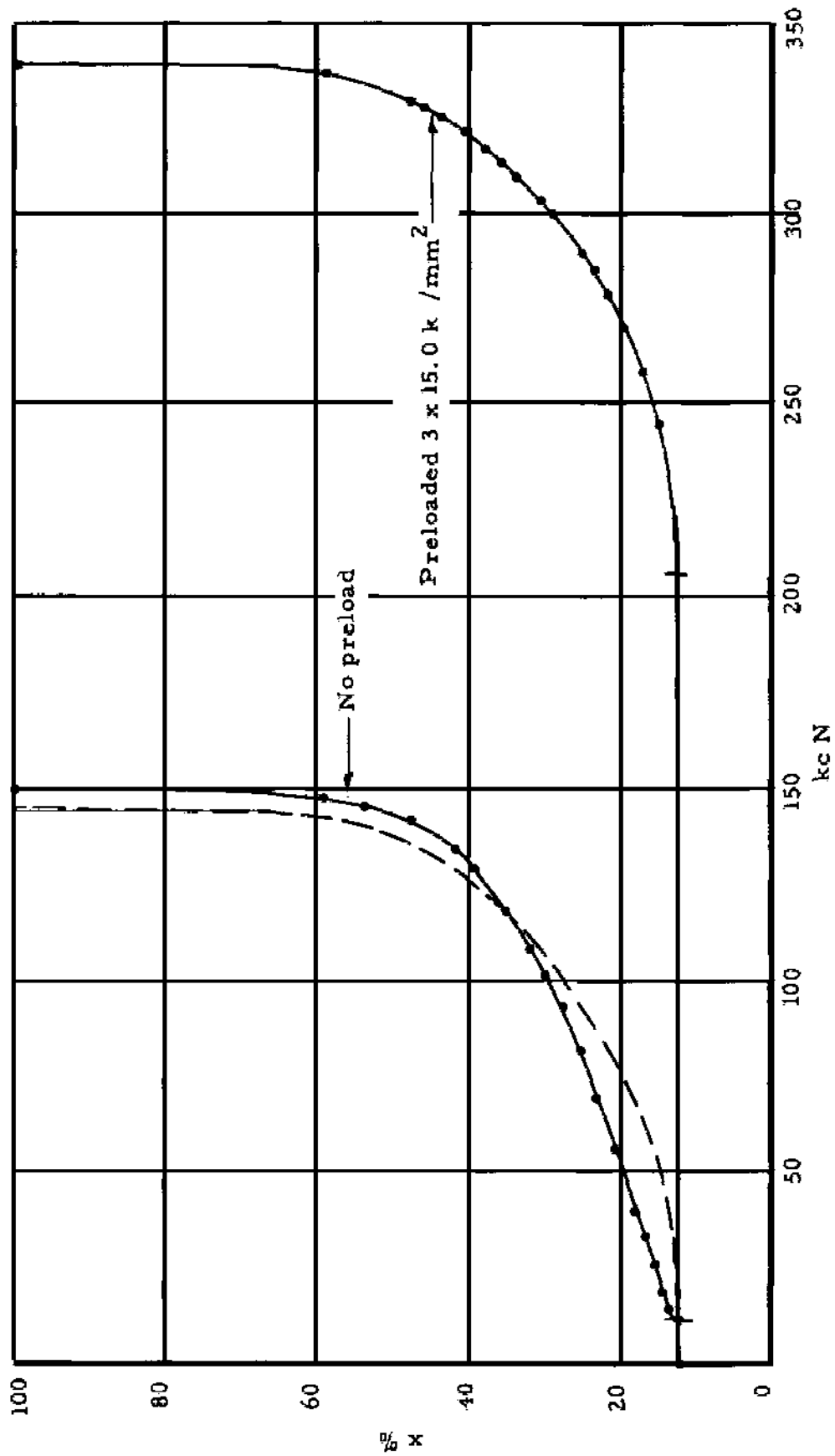


Figure 10. Series 7.0/170.6/12.1/2x without and with Preload ( $3 \times 15.0 \text{ kg/mm}^2$ ) Plotted on Linear Scales. Mat 24S-T.

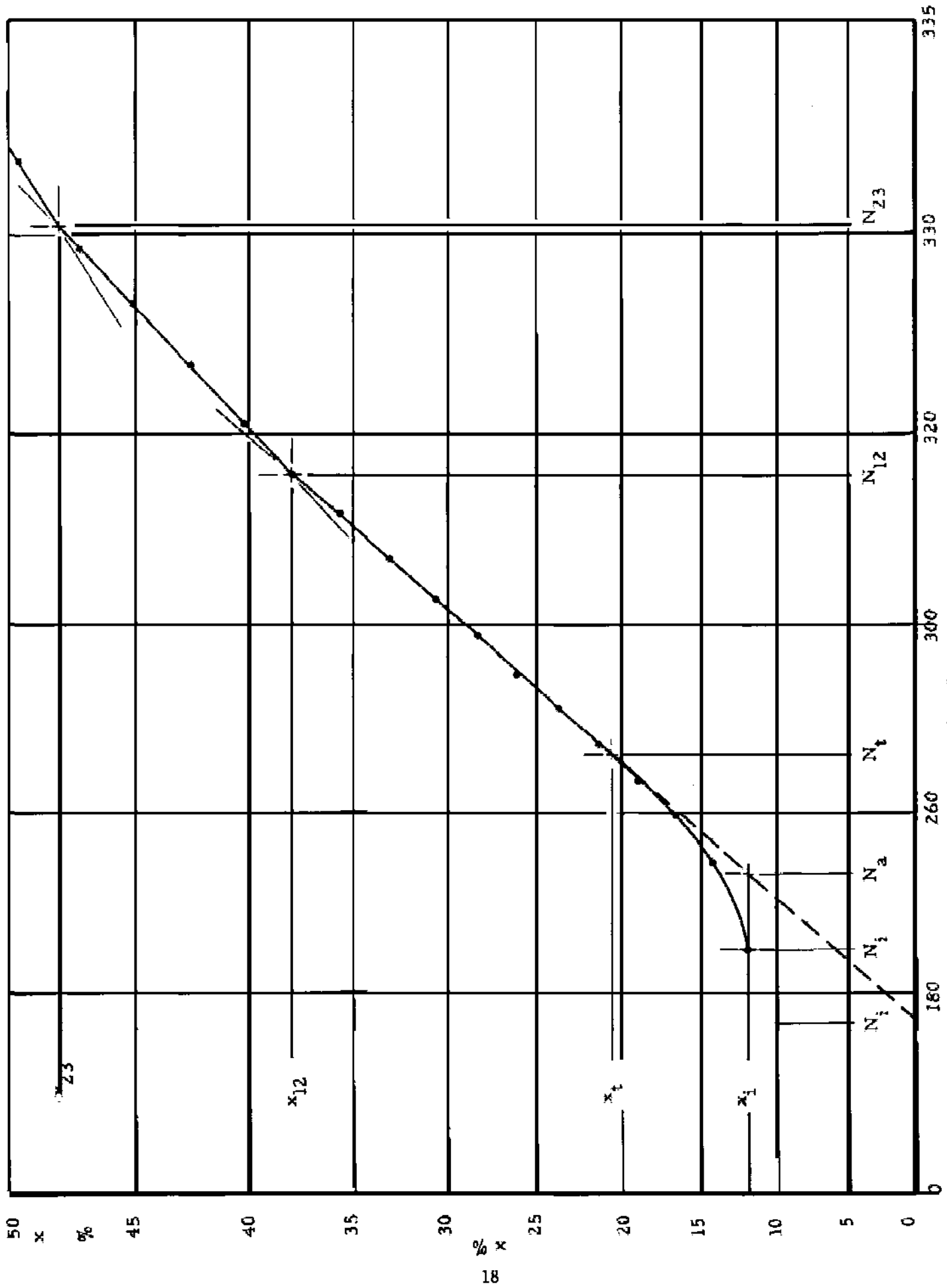


Figure 11. Series 7.0/170.6/12.1/2x Preload;  $\sigma_j = 8.0$ ,  $N_1 = 204$  kc



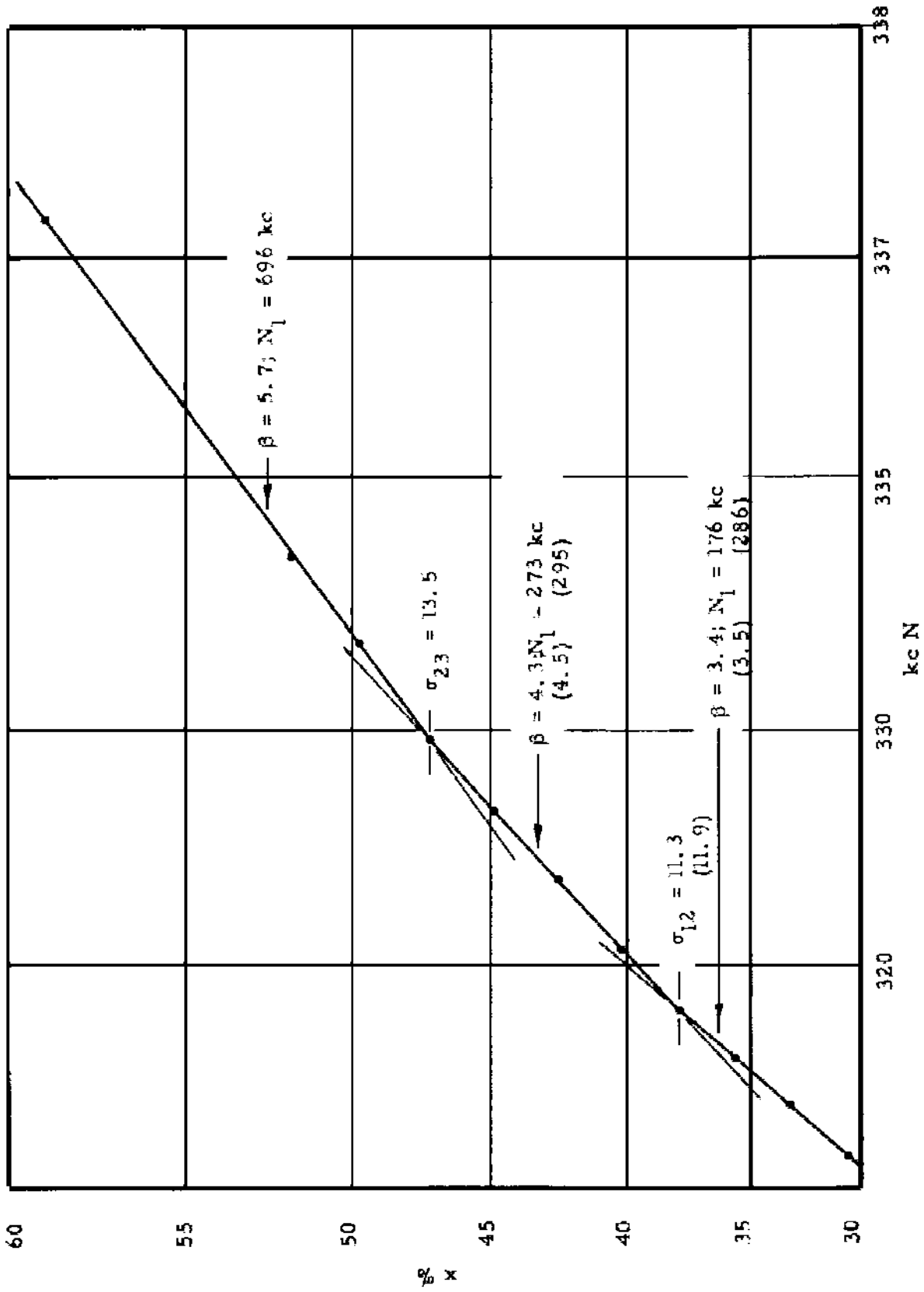


Figure 12. Series 7.0/170.6/12.1/2x Preloaded; Components 1, 2, and 3

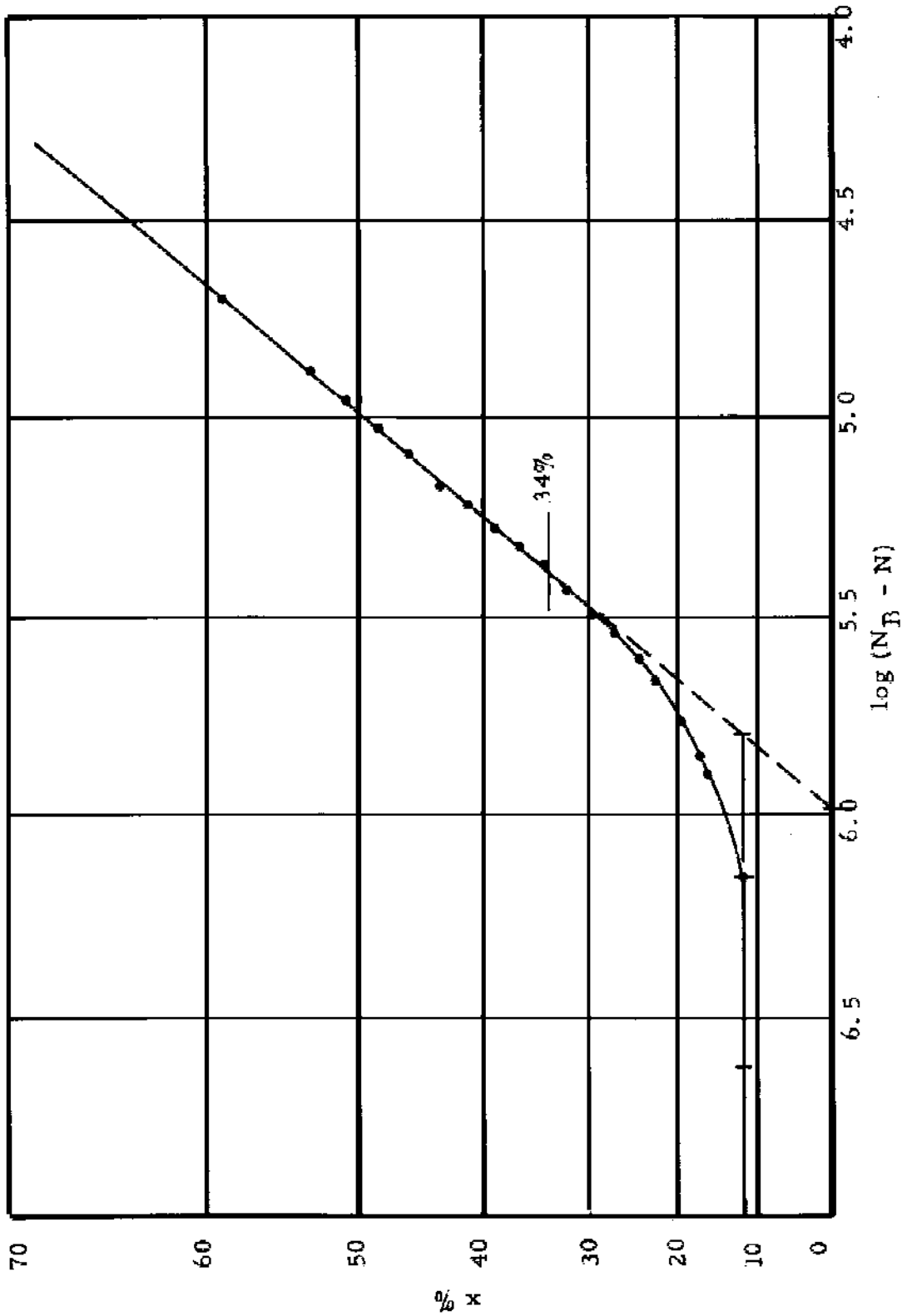


Figure 13. Series 3.5/170.6/12.1/2x;  $\sigma_i = 4.0$ ,  $N_i = 3,084$  kc. Mat. 24S-T

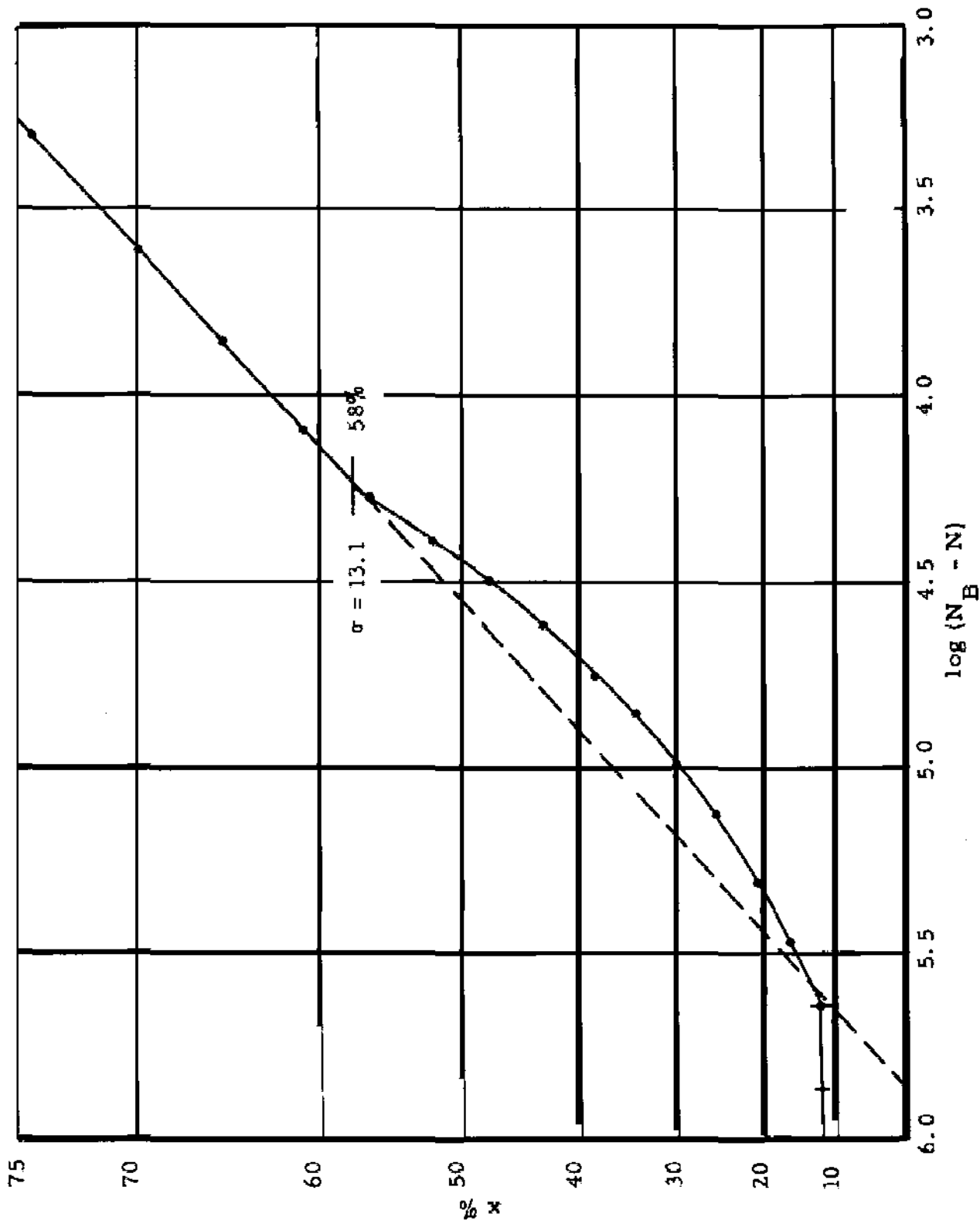


Figure 14. Series 5.5/45.0/12.2/2x;  $\sigma_j = 6.3$ ,  $N_i = 280$  kc. Mat. 245-T

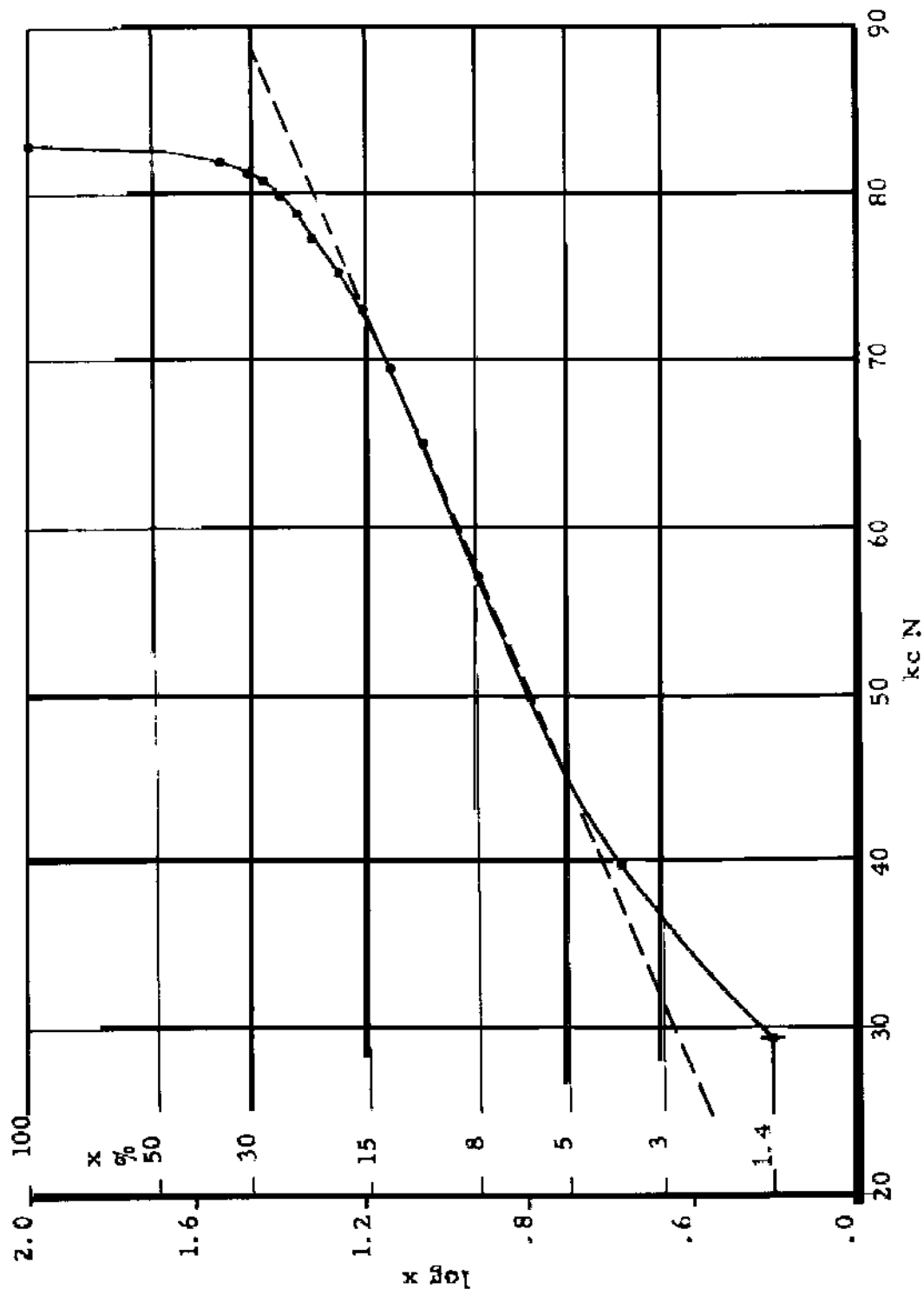


Figure 15. Series 11.8/170.6/1.4/2 sA Plotted on Log x ÷ N Scales. Mat. 24S-T

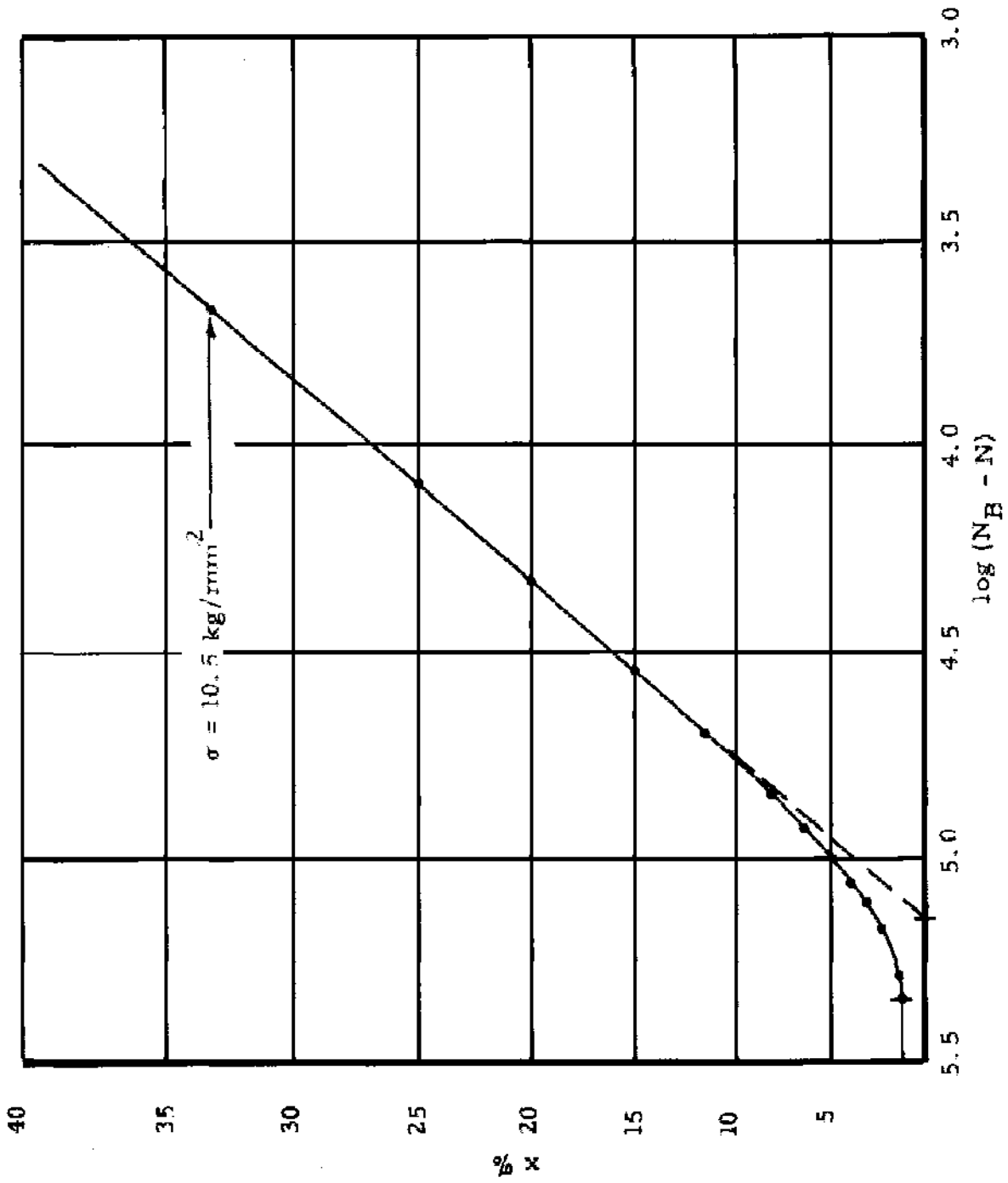


Figure 16. Series 7.0/304.8/1.0/2 s. Data from Illg and McEvily, NASA TN D-52, Mat. 2024-T3, S<sub>0</sub> = 6.00 ksi, R = -1